International Journal for Housing Science and Its Applications
Publish August 6, 2025. Volume 46, Issue 3 Pages 7731-7743

https://doi.org/10.70517/ijhsa463663

Research on the design of online monitoring system for transmission towers based on Internet of Things (IoT) platform

Liang'an Yao[1,*], Jingjia Shi[1], Chun Wang[1], Jun Liu[1] and Juan Du[1]
[1] State Grid Shanxi Electric Power Company Jinzhong Power Supply Company, Jinzhong, Shanxi, 030600, China
Corresponding authors: (e-mail: 13935413809@163.com).

Abstract The tilting of transmission towers may seriously threaten the normal operation of power grids. In this study, an online monitoring system for transmission towers based on the Internet of Things platform is designed, which aims to ensure the safe operation of the power grid by real-time monitoring of the tilting status of the towers and the surrounding meteorological environment. The system adopts a variety of sensors and ZigBee wireless communication technology, and transmits the data to the monitoring center through the on-site monitoring base station, which is able to realize remote real-time monitoring. Aiming at the problem of low-cost inertial measurement unit (IMU) accuracy in the existing monitoring system, this paper proposes an improved adaptive hybrid filtering algorithm (Sage-Husa), which is experimentally verified to effectively improve the stability and accuracy of the system. In the static experiments, the standard deviation of the Sage-Husa algorithm in the X-axis, Y-axis and Z-axis is 0.018, 0.0073 and 0.018, respectively, which shows a better noise reduction effect. In the dynamic experiments, evaluated using the root mean square error (RMSE), the RMSE of the Sage-Husa algorithm is 0.00154°/s (gyroscope) and 0.00305 m/s² (accelerometer), which shows better performance compared to other algorithms. The system designed in this paper can effectively improve the accuracy and reliability of tilt state monitoring of transmission towers, and has a wide range of application prospects.

Index Terms transmission tower, online monitoring, internet of things, tilt state, Sage-Husa, filtering algorithm

I. Introduction

With the continuous development of social economy, the electric power industry has become one of the most important basic industries in modern society [1]. With the expansion and complexity of the power grid, the cost and workload of transmission line maintenance has been increasing, which brings new challenges to the production and operation of power enterprises and social and economic development [2], [3]. As we all know, transmission line is a large system, involving countless transmission towers, the transmission tower online monitoring system based on the Internet of Things platform has a powerful and stable analysis, statistics and display functions [4]-[6]. The most important thing is to be able to intuitively give real-time status of transmission towers alarm notification, which can solve accidents or hidden dangers in a timely manner to ensure the stable operation of transmission lines [7], [8].

Traditional transmission towers are difficult to apply to the current needs due to the low precision of monitoring equipment, installation difficulties, poor anti-interference ability and other problems [9], [10]. In contrast, the online monitoring system of transmission pole tower based on IoT platform has the advantages of simple operation, high precision, real-time monitoring, and fast processing speed, which can complete the collection of electrical parameters of transmission lines, digital processing, conversion of analog signals, and wireless transmission, which can effectively improve the precision and stability of the sensors, and realize the real-time monitoring and prediction of the lines [11]-[14]. In addition, the design of online monitoring system of IoT provides ideas for solving the problems of insufficient network communication capacity and insufficient load capacity of traditional equipment, which can realize higher network bandwidth and transmission efficiency and improve the stability and reliability of the system [15]-[18]. It provides timely and accurate line fault information for electric power enterprises, and provides strong technical support and guarantee for the safe operation and management of transmission lines.

With the development of society, power grid plays an indispensable role in daily life. As an important part of the power grid, the inclined state of transmission towers is crucial to the safe operation of the power grid. Traditional transmission tower inspection methods mostly rely on manual inspection, which is not only inefficient, but also unable to cope with the challenges posed by complex terrain and extreme climate. Especially in remote areas or harsh environments, the feasibility and accuracy of manual inspection are greatly limited. Therefore, how to utilize

advanced technical means, especially the Internet of Things (IoT) technology, to realize real-time monitoring of transmission towers has become an urgent problem in the current power industry.

In order to solve the above problems, this paper proposes an online monitoring system for transmission towers based on IoT platform. The system collects the tilt data of the pole tower in real time by installing sensors on the pole tower and transmits these data to a remote monitoring center through wireless communication, thus realizing real-time monitoring of the tilt status of the pole tower. The system adopts low-power IMU sensors and combines with ZigBee wireless communication technology to ensure the stability and reliability of data transmission. Meanwhile, in order to overcome the accuracy problems in traditional IMU measurement, this paper proposes a program based on an improved adaptive hybrid filtering algorithm (Sage-Husa), which can effectively reduce the noise and improve the measurement accuracy. Through experimental verification, the system not only meets the practical application requirements, but also improves the monitoring efficiency and reduces the cost invested by the power company in the inspection process.

II. Transmission tower online monitoring system design

With the acceleration of power grid construction and the advancement of market economy, the tilting of transmission line towers is increasingly harmful to the safe and normal operation of the power grid. As an emerging network technology for intelligent identification, localization, tracking, monitoring and management, the deep integration of IoT platform with power grid construction is the inevitable result of the development of information and communication technology to a certain stage. This chapter will take the IoT platform as the basis to design the transmission tower online monitoring system based on the principles of reasonable, practical, feasible and reliable.

II. A. General structure of the system

The system consists of on-site multifunctional monitoring base station (including control system, multiple monitoring sensors, solar power supply system, modules, modules, etc.) and monitoring center software, and the overall system structure is shown in Fig. 1. The on-site multifunctional monitoring base station is installed on the pole tower of the transmission line and powered by the solar power supply system, which is used to process the real-time monitoring data as well as the warning and alarm information, and sends the processed real-time on-site monitoring data to the module through the ZigBee wireless communication system, and then sends it to the upper computer monitoring center through the module. The module is responsible for summarizing the on-site monitoring data and collecting data information from adjacent towers, avoiding placing modules on each tower and saving costs. The module is the bridge connecting the field and the upper computer. The monitoring center is the core of the system, which is responsible for communicating with the on-site multi-functional monitoring base station (including sending control commands, receiving real-time on-site monitoring data transmitted back from on-site monitoring terminals as well as early warning and alarm information), storing the relevant data of all kinds of monitoring information into the database, managing all kinds of monitoring information, and providing application services to the remote customers of the system.

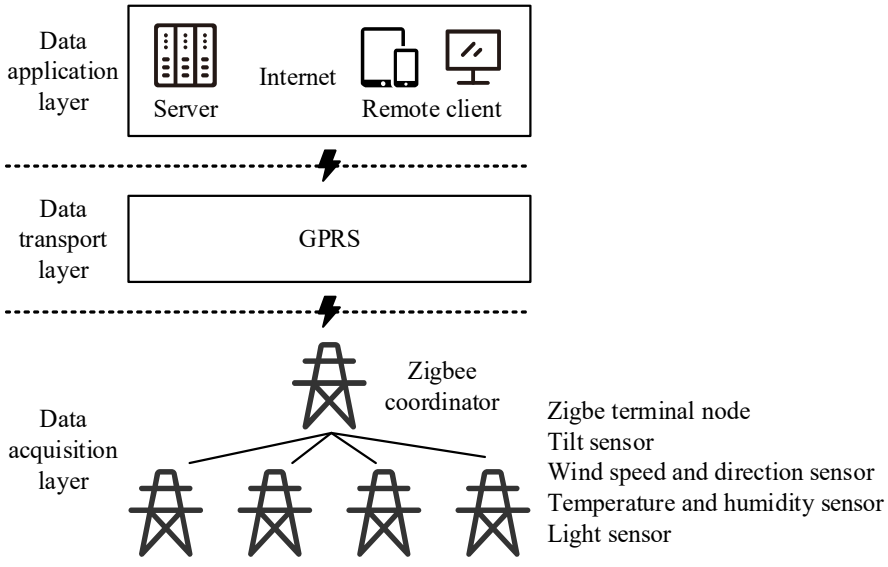

Figure 1: The structure of transmission tower on-line monitoring system

II. B.System characteristics

In this paper, the system is based on the Internet of Things communication technology and sensor technology as the core, set tower tilt monitoring temperature and humidity monitoring and other functions in one; the sensor itself is the node of communication, with self-organized wireless network as the medium of information transfer, so as to solve the difficulties of field communication. Each sensor has different functions, but can be added on demand, free combination, cost savings, improved efficiency, can achieve fast and accurate fault analysis, in line with the requirements of intelligent power transmission. This system has the following characteristics:

(1) The system adopts online monitoring, online diagnosis, online command and other functions of the modular structure, is a remote tower tilt online monitoring, online supervision and prevention of multi-functional integration of a comprehensive system, through a set of systems will be able to realize the transmission line tower online monitoring, able to complete the daily operation of the transmission line remote patrol management, maintenance and rescue operations remote command, remote fault analysis and diagnosis of a variety of tasks.

(2) The system operates in a multi-level and distributed way, and complies with the relevant technical standards of the State Grid Corporation, which can forward real-time on-site monitoring data and warning and alarm information to the transmission line monitoring center of the provincial power company in real time, with strong technical specifications and compatibility, and can form a remote online monitoring system for the operating status of transmission line towers of the provincial power company. The bottom-end data transmission pro-application method ensures the stability of data and saves the system cost; meanwhile, the microcontroller control system adopts low-power design to ensure the sustainable operation of the equipment.

(3) Using the operator's existing network to build a remote data transmission channel, which can meet the reliable operation under different communication environments in the field, and realize the transmission line online monitoring system monitoring center can monitor the data in the remote site in real time. The system is constructed with multi-layer shielding technology, and the enclosure and sensor shell are made of anti-magnetic metal materials, which can effectively shield electromagnetic interference.

(4) Strong environmental adaptability, the system's resistance to low temperatures and other harsh conditions, anti-electromagnetic interference performance has experienced long-term laboratory tests and field operation field tests. The system has a unified platform with scalable monitoring functions, which can correspond to fixed monitoring devices and mobile monitoring devices. The on-site multifunctional monitoring base station can be disassembled and moved, and installed in temporary construction sites such as construction sites, disaster areas, etc. It is applicable to transmission lines, substation equipment, stations and other occasions.

II. C.Role of the system

(1) The system can carry out remote on-line monitoring of the tilt data of transmission line towers and the surrounding meteorological environment, solving the problem that manual inspection cannot always reach the remote dangerous monitoring points in normal times and cannot reach them in time in emergency times, and realizing all-weather remote automatic monitoring.

(2) The system adopts the combined power supply of solar energy and storage battery, which ensures that the system can run continuously for a long time in the outdoor environment.

(3) The overall design of the system program is completed, and various types of sensors are integrated into the network, including the inclination measurement part and the small space weather station part. The system can realize remote online monitoring of micro-meteorological parameters (temperature and humidity, wind speed, wind direction) around the transmission line, providing objective conditions for predicting other parameters of the transmission line.

(4) The system realizes low-power design of hardware and software, and the effect of low power consumption is obvious.

(5) The system can real-time forward real-time on-site monitoring data to the monitoring center of high-voltage transmission lines of provincial power companies, as well as early warning information, in order to form a remote on-line monitoring system for the operation status of high-voltage transmission lines of provincial power companies.

(6) The system can realize remote client access, set up the server and client to facilitate the management and resource sharing of various units.

III. Improvement of transmission tower inclination measurement methods

Aiming at the problems of low measurement accuracy, easy dispersion of attitude solution and poor stability of tower inclination measurement by low-cost inertial measurement unit (IMU) in the online monitoring system for transmission towers, this chapter proposes an inclination measurement method for transmission towers based on improved adaptive hybrid filtering algorithm.

III. A. Attitude solving

In order to characterize the attitude of transmission towers, it is first necessary to link the MEMS-IMU coordinate system mounted on the towers with the known ground coordinate system. The carrier coordinate system (b-system) and the navigation coordinate system ($_n$-system) are defined, and the traditional "north-east sky" is chosen as the base coordinate system, i.e., the $X_nY_nZ_n$-axis represents the east, the north and the sky, respectively. The Euler angles are usually used to define the angles around the three axes of direction, i.e., traverse roll angle φ, pitch angle γ, and heading angle ψ .

In order to further characterize the attitude of the tower, it is also necessary to determine the relative relationship between the carrier coordinate system and the navigation coordinate system. Considering the computational volume and efficiency of using Euler angles to participate in attitude solving, the quaternion method, which has obvious advantages in terms of computational volume and accuracy and can avoid the "singularity" problem, is chosen. The expression of quaternion is defined as:

$$Q(q_0,q_1,q_2,q_3)=q_0+q_1i+q_2j+q_3k \tag{1}$$

In equation (1): q_0,q_1,q_2,q_3 are real numbers; i,j,k are the bases of the imaginary number space. It can be seen that the quaternions are vectors, and changing the value of q allows one to use them to describe arbitrary gestalt information in space.

The expression for the relationship between the two coordinate systems is:

$$\begin{bmatrix} X_b \\ Y_b \\ Z_b \end{bmatrix}=C_n^b(\varphi,\gamma,\psi)\begin{bmatrix} X_n \\ Y_n \\ Z_n \end{bmatrix} \tag{2}$$

In Eq. (2): C_n^b is the transformation matrix between the two coordinate systems; it is expressed in quaternions as:

$$C_n^b=\begin{bmatrix} q_0^2+q_1^2-q_2^2-q_3^2 & 2(q_1q_2-q_0q_3) & 2(q_0q_3+q_1q_2) \\ 2(q_1q_2-q_0q_3) & q_0^2-q_1^2+q_2^2-q_3^3 & 2(q_2q_3+q_0q_1) \\ 2(q_1q_3-q_0q_2) & 2(q_0q_1+q_2q_3) & q_0^2-q_1^2-q_2^2+q_3^2 \end{bmatrix} \tag{3}$$

Then the 3 attitude angles can be expressed in quaternions as:

$$\begin{cases} \varphi=\arcsin\left[-2(q_0q_2+q_1q_3)\right] \\ \gamma=\arctan\left[\dfrac{2(q_2q_3-q_0q_1)}{q_0^2-q_1^2-q_2^2+q_3^2}\right] \\ \psi=\arctan\left[\dfrac{2(q_1q_2-q_0q_3)}{q_0^2+q_1^2-q_2^2-q_3^2}\right] \end{cases} \tag{4}$$

$$\dot{q}_b^n=\frac{1}{2}q_b^n\otimes\omega \tag{5}$$

In Eq. (5): $\dot{q}_b^n$ is the quaternion of the b-system transformed into the $_n$-system; $\dot{q}$ is the derivative of the quaternion: $\otimes$ denotes the quaternion multiplication: $_\omega$ is the output of the gyroscope. Substitution gives:

$$\begin{bmatrix} \dot{q}_0 \\ \dot{q}_1 \\ \dot{q}_2 \\ \dot{q}_3 \end{bmatrix}=\frac{1}{2}\begin{bmatrix} 0 & -\omega_x & -\omega_y & -\omega_z \\ \omega_x & 0 & \omega_z & -\omega_y \\ \omega_y & -\omega_z & 0 & \omega_x \\ \omega_z & \omega_y & -\omega_x & 0 \end{bmatrix}\begin{bmatrix} q_0 \\ q_1 \\ q_2 \\ q_3 \end{bmatrix} \tag{6}$$

In Eq. (6): assuming that the current moment is t and the sampling period is T the quaternion of the next moment can be obtained as:

$$q(t+T)=q(t)+\frac{T}{2}q(t)\otimes\omega \tag{7}$$

Eq. (7) is the quaternion of the next moment, which is substituted into Eq. (3) to obtain the updated C_n^b. The tower attitude angle at the latest moment is then obtained from Eq. (4).

III. B. Algorithmic studies

After solving the tower attitude angle using the quaternion method, the noise and error of gyroscopes and accelerometers need to be reduced at the level of sensor fusion algorithms.

III. B. 1) Traditional complementary filtering algorithms

The input data to the complementary filter is obtained from gyroscope and accelerometer measurements.The schematic diagram of the complementary filter is shown in Fig. 2, and the transfer function expression is:

$$\begin{cases} F_1(s)=\dfrac{k_p s+k_i}{s^2+k_p s+k_i} \\ F_2(s)=\dfrac{s^2}{s^2+k_p s+k_i} \end{cases} \tag{8}$$

It can be seen that the sum of $F_1(s)$ and $F_2(s)$ is 1 and the relation is complementary.

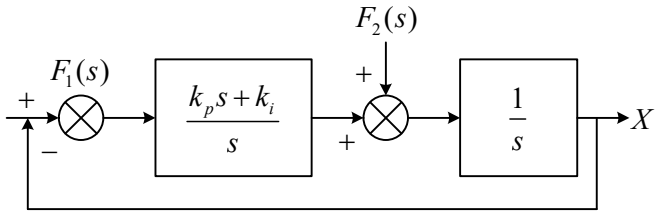

Figure 2: Overall structure diagram of the system

To obtain a good complementary filtering effect, it is necessary to select a suitable cutoff frequency, which is realized by choosing the control parameters k_p and k_i, the two parameters represent the trust weights on the gyroscope measurements and accelerometer strategy values, respectively.

III. B. 2) Improved complementary filtering algorithm

In the actual environment, the tower is greatly affected by the wind and the dancing tension of the power line caused by the wind, and a set of fixed control parameters is difficult to cope with different wind speed situations, which will lead to the deviation of the attitude estimation results. Therefore, we adopt the strategy of taking the data measured by the accelerometer as the benchmark for judging the motion situation, and divide the judgment results into 3 situations: no acceleration state, low acceleration state, high acceleration state, and reduce the trust weight of the accelerometer in turn.

The PI parameters are adjusted according to the 3 situations to realize the adaptive improvement of complementary filtering.

Let the combined acceleration of the carrier be:

$$a_{total}=\left|\sqrt{a_x^2+a_y^2+a_z^2}-g\right| \tag{9}$$

In Eq. (9): a_x, a_y, a_z are the accelerometer outputs; g is the gravitational acceleration.

Setting the low acceleration state threshold as L and the high acceleration state threshold H as 0.01g, there are:

$$L=\sigma_x^2+\sigma_y^2+\sigma_z^2 \tag{10}$$

In Eq. (10): $\sigma_x,\sigma_y,\sigma_z$ is the standard deviation of the noise when the accelerometer is stationary.

The judgment criteria for the 3 acceleration cases are as follows.

(1) When $a_{total}\le L$, the tower is in the no-acceleration state, at this time take $k_p=0.5$.

(2) When $L<a_{total}\le H$, the tower is in a low acceleration state, $k_p=\dfrac{1}{1+a_{total}}$.

(3) When $a_{total}>H$, the tower is in high acceleration state, at this time, the attitude angle obtained by the accelerometer will have a large error and no reference meaning, so take $k_p=0$.

III. B. 3) Sage-Husa adaptive filtering

The classical Kalman filter algorithm and the extended Kalman filter algorithm need to satisfy the condition that the statistical characteristics of the system noise are known when they are used, while in the actual application, the noise generated by the tower by various environmental influences is unknown, and the solution value is likely to generate dispersion. Therefore, the Sage-Husa Kalman filter with time-varying noise statistics as the core is used [19]. Let the state equation and the measurement equation be:

$$\begin{cases} X_k = AX_{k-1}+W_{k-1} \\ Z_k = HX_k+V_k \end{cases} \tag{11}$$

In Eq. (11): X_k is the state variable matrix; Z_k is the measurement variable matrix; A is the transfer matrix from $k-1$ moments to k moments; H is the observation matrix at k moments; and W_{k-1} and V_k are the state noise matrix and the measurement noise matrix respectively.

The basic steps of the algorithm update are:

$$\begin{cases} \hat{X}_{(k|k-1)}=A_{(k|k-1)}\hat{X}_{k-1}+\hat{q}_{k-1} \\ P_{(k|k-1)}=A_{(k|k-1)}P_{k-1}A_{(k|k-1)}^T+\hat{Q}_{k-1} \\ K_k=\dfrac{P_{(k|k-1)}H_k^T}{H_kP_{(k|k-1)}H_k^T+\hat{R}_k} \\ e_k=Z_k-H_k\hat{X}_{(k|k-1)}-\hat{r}_{k-1} \\ \hat{X}_k=\hat{X}_{(k|k-1)}+K_ke_k \\ P_k=(I-K_kH_k)P_{(k|k-1)} \end{cases} \tag{12}$$

In Eq. (12): $P_{(k|k-1)}$ is the covariance associated with the a priori estimate $X_{(k|k-1)}$ at moment k, with subscript $(k|k-1)$ denoting the a priori estimate at moment k, and subscript $(k|k)$ denoting the a posteriori estimate at moment k; $\hat{r}_k$ and $\hat{q}_k$ are estimates of the expectation of the measurement error and the systematic error, respectively; K_k is the Kalman gain at the k moment; Q,R is the covariance matrix of the noise; I is the unit matrix.

The noise estimator with time-varying performance is as follows:

$$\begin{cases} \hat{r}_k=(1-d_k)\hat{R}_{k-1}+d_k[Z_k-H_k\hat{X}_{(k|k-1)}] \\ \hat{R}_k=(1-d_k)\hat{R}_{k-1}+d_k[e_ke_k^T-H_kP_{(k|k-1)}H_k^T] \\ \hat{q}_k=(1-d_k)\hat{q}_{k-1}+d_k[\hat{X}_k-A_{(k|k-1)}\hat{X}_{k-1}] \\ \hat{Q}_k=(1-d_k)\hat{Q}_{k-1}+d_k[K_ke_ke_k^TK_k^T+P_k-A_{(k|k-1)}P_{k-1}A_{(k|k-1)}^T] \\ d_k=(1-b)/(1-b^{k+1}) \end{cases} \tag{13}$$

In Eq. (13): $\hat{R}_k$ and $\hat{Q}_k$ are the estimates of measurement error and systematic error covariance, respectively; d_k is the forgetting factor, in which the value of b is in the range of (0, 1), and that of d_k is [0.95, 0.99], adjusted to 0.95 after several values. 0.99], which was adjusted to 0.95 after several value adjustments.

By Sage-Husa adaptive filtering algorithm, the estimates of the measurement noise $\hat{R}_k$ and system noise $\hat{Q}_k$ can be obtained. From Eq. (12), the updating formula of the noise contains the new interest vector e_k, it can be seen that any abnormality in the updating process will affect the accuracy of the noise computation, which will lead to the deterioration of the filtering effect; and the updating of the statistical characteristics of the noise needs to be repeated once for each iteration, which is a large amount of computation. Therefore, the Sage-Husa adaptive algorithm needs to be improved.

III. B. 4) Improved Sage-Husa adaptive filtering

In the process of filtering calculation, the statistical properties of the actual e_k should be consistent with its theoretical statistical properties, so it is necessary to constantly test the new interest term and determine whether the actual and theoretical properties are consistent, when the actual e_k is not consistent with the original noise $\hat{R}_k, \hat{Q}_k$, it indicates that there is an abnormality in the filtering calculation process. Consistency is an indication that the filtering calculation process is anomalous, with a high probability of divergence, at which point the estimate is updated. Generally, the square of e_k is used as a criterion for filtering anomaly:

$$e_k e_k^T \le \xi tr \mid E(e_k e_k^T) \mid \tag{14}$$

In Eq. (14): ξ is the reserve coefficient, which takes the value ≥ 1, and tr is the trace of the matrix. The left side of the inequality sign indicates the actual error and the right side indicates the product of the theoretical error and the reserve coefficient. The fact that Eq. (14) holds indicates that the filtering converges.

Associating the criterion with the second term of Eq. (11) and the fourth term of Eq. (12) yields the new interest formula as:

$$e_k = H_k[X_k - \hat{X}_{(k|k-1)}] + V_k \tag{15}$$

In Eq. (15): e_k is uncorrelated with $[X_k - \hat{X}_{(k|k-1)}]$ and the covariance of the noise V_k is R_k, which yields $E(e_k e_k^T)$ calculated as:

$$E(e_k e_k^T) = H_k P_{(k|k-1)} H_k^T + R_k \tag{16}$$

The strictest convergence criterion is when the reserve coefficient takes the value of 1. Substituting Eq. (11) into Eq. (8) yields:

$$e_k e_k^T \le H_k P_{(k|k-1)} H_k^T + R_k \tag{17}$$

Eq. (17) is the convergence criterion of the Sage-Husa adaptive filtering algorithm, and when the filtering process does not satisfy the criterion it is updated with Eq. (18), i.e:

$$P_{(k|k-1)} = S_k A_{k-1} P_{(k-1|k-1)} A_{k-1}^T + Q_{k-1} \tag{18}$$

In Eq. (18): S_k is the filter weighting coefficient, which takes the value of 1. The update of K_k can be realized by the change of $P_{(k|k-1)}$, which in turn prevents the filter divergence.

III. C. Simulation experiment of transmission tower inclination measurement

In this chapter, the effectiveness of the proposed transmission tower inclination measurement method based on the improved adaptive hybrid filtering algorithm (Sage-Husa) will be tested through static turntable experiments and dynamic experiments under laboratory conditions.

III. C. 1) Static experimental simulation analysis

The IMU adopts MPU6050 with built-in three-axis gyroscope and three-axis accelerometer, which is firstly calibrated and benchmarked before using the IMU. In the first stage of calibration, the scale factor and cross-sensitivity coefficient of the gyroscope are determined at a given value of rotational angular velocity. In the second stage of

calibration, the zero point of the gyroscope is offset and the sensitivity coefficients of the zero point of the gyroscope signal to the acceleration sensitivity are determined for different positions of the gyroscope with respect to the gravitational acceleration vector. The output signals of the calibrated gyroscope were read in 10 minutes and imported into Matlab to calculate the standard deviation of the array elements. The Z-axis of the gyroscope and accelerometer has the largest zero offset and noise standard deviation, while the Y-axis has the smallest zero offset and noise standard deviation.

The results of the Allan standard deviation analysis of the X, Y and Z axes of the MEMS gyroscope and accelerometer under static conditions are specifically shown in Table 1. The dynamic test results of BI with ARW of Allan variance show that the Sage-Husa adaptive filtering algorithm in this paper can effectively reduce the ARW and BI noise, while the mean value remains unchanged. Comparing the Allan standard deviation values of each algorithm, the smaller the value indicates that the overall data is more stable, because the Sage-Husa adaptive filtering algorithm of this paper removes the data with large random noise in the measurement data of IMU, so the data stability is higher and the data accuracy is also improved as a result, and the conclusion shows that the Sage-Husa adaptive filtering algorithm of this paper has the advantage of dealing with the uncertainty of the model of the The conclusion shows that the Sage-Husa adaptive filtering algorithm in this paper has better adaptive performance and noise reduction ability when dealing with the uncertainty model filtering problem.

Table 1: Allen standard deviation analysis results

Algorithm	-	ARW($^\circ/\sqrt{h}$)	BI($^\circ/\sqrt{h}$)	Allan standard deviation($^\circ/\sqrt{h}$)
Raw data of MEMS gyroscope	X axis	1.64×10^{2}	0.82×10^{2}	0.64×10^{2}
	Y axis	3.24×10	0.78×10	0.1×10^{-1}
	Z axis	3.82×10	0.92×10	0.07×10^{-1}
SHAKF	X axis	0.77×10^{-2}	0.35×10^{-1}	0.13×10^{-2}
	Y axis	0.37×10^{-2}	0.11×10^{-1}	0.51×10^{-2}
	Z axis	0.37×10^{-1}	0.4×10^{-2}	0.54×10^{-2}
ARKF	X axis	0.48×10^{-2}	0.18×10^{-1}	1.13×10^{-3}
	Y axis	0.44×10^{-2}	0.14×10^{-1}	0.42×10^{-3}
	Z axis	0.32×10^{-2}	0.3×10^{-1}	0.42×10^{-2}
Sage-Husa	X axis	0.18×10^{-2}	0.6×10^{-2}	3.89×10^{-3}
	Y axis	0.73×10^{-3}	0.25×10^{-3}	0.51×10^{-4}
	Z axis	0.18×10^{-2}	0.87×10^{-3}	0.37×10^{-4}

III. C. 2) Dynamic experimental simulation analysis

To obtain data from the dynamic MEMS-IMU, the rotation of the rate table was varied in a stepwise manner starting from zero degrees per second. The root mean square error (RMSE) was used as an evaluation criterion to test the filter performance under dynamic conditions. The RMSE was calculated for each step of the rotating signal for 10000 samples, and the root mean square error of the MEMS-IMU sensor is specifically shown in Table 2. From the Allan variance results and bias drift of the filtered signals listed in the table, it can be seen that the Sage-Husa adaptive filtering algorithm in this paper is more responsive and the results are smoother, and it effectively reduces the zero-bias instability and angular random wandering in the IMU. In the case of Sage-Husa adaptive filtering algorithm in this paper, the random noise such as angular random wander and bias instability is significantly reduced.

Table 2: MEMS-IMU sensor root mean square error

-	RMSE of gyroscope(°/s)	RMSE of accelerometer(m/s^2)
Raw data	5.49×10^{-2}	6.41×10^{-2}
SHAKF	1.39×10^{-2}	1.27×10^{-2}
ARKF	2.05×10^{-3}	4.34×10^{-3}
Sage-Husa	1.54×10^{-3}	3.05×10^{-3}

Overall, the Sage-Husa adaptive filtering algorithm in this paper has good performance in both static and dynamic conditions, and the transmission tower inclination measurement method based on the improved adaptive hybrid filtering algorithm proposed in this paper can play an effective role in the transmission tower inclination measurement work.

IV. Improvement of transmission tower tilt state identification method

Aiming at the problems such as the difficulty and low accuracy of the transmission tower online monitoring system in extracting the structural state information of transmission towers, this chapter proposes a tilt state recognition scheme for transmission tower tilting based on the variational modal decomposition optimized by the Northern Eagle Algorithm (NGO-VMD) and the Long Short-Term Memory (LSTM) neural network [20], [21].

IV. A. Variational modal decomposition

VMD has good frequency division characteristics, and its application to the vibration signal processing of transmission towers can decompose the tower's inherent frequency information of each order under vibration.

Variable modal decomposition decomposes the original signal S into IMFs of specified order m with different center frequencies, which is calculated as follows:

$$\begin{cases} \min\left\{\sum_{m}\| \partial t[(\delta(t)+j/\pi t)u_m(t)]e^{-j\omega_m t}\|_2^2\right\} \\ s.t.\sum_{m=1}^{M}u_m(t)=S \end{cases} \tag{19}$$

where, ∂t is the function taking the partial derivative with respect to time t; $\delta(t)$ is the impulse function; M is the maximum number of decomposition layers; ω_m is the center frequency of the m th order; u_m is the IMF component of the m th order; $e^{-j\omega_m t}$ is the mixing operator to modulate the center band of the spectrum of each order; $\|\cdots\|_2^2$ is the square of the 2-parameter of the frequency gradient, which is used to estimate the bandwidths of the components of each order. Eq. (1) also suffers from the constraint problem, and the variational modal decomposition can be accomplished by the Lagrange multiplier algorithm and the alternating direction multiplier method (ADMMM) by alternating iterative optimization search.

From the above theory, it can be seen that the VMD requires some specific input parameters before it can be applied to signal decomposition. The first input parameter is the number of decomposition layers K of the VMD, and the second input parameter is the penalty factor α that determines the bandwidth of the IMF component. If the parameters are not chosen properly, it will cause under-decomposition and over-decomposition phenomena, which will seriously affect the decomposition of the original signal.

IV. B. Northern Eagle Algorithm

NGO is a multi-objective optimization algorithm based on the predation strategy of the northern goshawk, which has the advantages of strong optimization ability and fast convergence speed. In VMD, the parameters K and α need to be determined artificially and are more difficult, while the optimization algorithm can be used to solve this problem, the northern goshawk predation mainly undergoes 2 steps, which are identifying the prey and pursuing the prey.

1) The northern goshawk will randomly select a prey and quickly attack when hunting, this process is to explore and select the optimal prey area, so that the algorithm can more accurately and quickly identify the optimal area under the global search. The predation exploration behavior of the northern goshawk can be described as:

$$x_{i,j}^{new,P_1}=\begin{cases} x_{i,j}+r(P_{i,j}-Ix_{i,j}), F_{pi}<F_i \\ x_{i,j}+r(x_{i,j}-P_{i,j}), F_{pi}\geq F_i \end{cases} \tag{20}$$

where $x_{i,j}^{new,P_1}$ is the new position of the jth dimension of the i th northern goshawk in stage 1; $x_{i,j}$ is the position of the jth dimension of the i th northern goshawk; $P_{i,j}$ is the information about the position of the jth dimension of the prey of the i th northern goshawk; I is either a 1 or 2 of random integers; F_i is the fitness function representing the position of the i th northern pallid eagle; F_{pi} is the target value of the prey position information of the i th northern pallid eagle; and r is a random number on the interval [0, 1].

2) After determining the prey target, the northern goshawk will pursue the prey that is escaping with an assumed pursuit range radius R. The northern goshawk has a high predation speed and pursuit success rate, which makes the algorithm's ability for its local spatial optimization more significant. The pursuit process of the northern goshawk can be described by Eq. (21), and Eq. (22) describes the positional turnover of the northern goshawk:

$$x_{i,j}^{new,P_2} = x_{i,j} + R(2r-1)x_{i,j} \tag{21}$$

$$x_i = \begin{cases} x_i^{new,P_2}, & F_i^{new,P_2} < F_i \\ x_i, & F_i^{new,P_2} \geq F_i \end{cases} \tag{22}$$

where, R is the range radius of capture; x_i is the position of the i th northern pallid sturgeon; $F_i^{new,P2}$ is the value of the objective function based on the i th northern pallid sturgeon after the update of the 2nd stage; $x_i^{new,P2}$ is the new position of the i th northern pallid sturgeon after the update of the 2nd stage; $x_{i,j}^{new,P2}$ is the new position of the j th dimension of the i th Northern Pale Eagle in stage 2.

After going through the above two steps, which is equivalent to going through one iteration completely, the updated population member information is derived, and after going through the last loop, the final population member position information is the optimal value. From equation (20)(22), it can be seen that the population updating criterion of NGO is the size of F_i , and after setting up its fitness function F_i by the establishment criteria of parameter K and α in the theory of VMD, the K and α of the northern eagle algorithm will be used to select optimal parameters with input optimization searching range R in the VMD according to equation (3). Optimal parameter selection.The specific process of NGO-VMD is as follows.

(1) Obtain the vibration data of the tower;

(2) Set the parameter ranges of K and α in VMD and initialize the population of northern goshawk;

(3) Calculate the fitness function and select the parameter set for loop iteration using equation (21);

(4) Output the optimal parameters and run them into the VMD to produce the decomposition results of the NGO-VMD.

IV. C. Singular value decomposition

Through the NGO-VMD, a set of IMF functions reflecting the modal characteristics of transmission towers can be obtained, and in order to further accurately extract the key information of each order of IMF, the singular values can be used for characterization. Therefore, the IMF of each order is subjected to SVD, and the obtained singular value σ can characterize the important modal features of the IMF of this order.SVD is a matrix decomposition method, and some hidden information and weak information can be obtained in the separated state of the matrix. Assuming the matrix is X , its decomposition equation is:

$$X = USV^T \tag{23}$$

where, U,V is the orthogonal matrix; S is the singular value diagonal matrix.

According to the singular value decomposition formula and singular value theory, U,V is not unique and the matrix S has uniqueness, the singular value represents the important information characteristics of this matrix, when the signal perturbation phenomenon occurs, the singular value of it will not be a large change, so as to avoid the existence of randomness in the time series of the false characteristics of the time series, so that it is in the field of feature extraction has a strong stability and adaptability. That is to say, taking $[\hat{\sigma}_1, \hat{\sigma}_2, \ldots, \hat{\sigma}_{K-1}]$ as the feature vectors of the original signals can effectively reflect the state information of the tower structure.

IV. D. Long and short-term memory neural networks

The vibration signals of transmission towers can be obtained as a set of singular value vectors through NGO-VMD with singular value decomposition, and how to reflect the overall structural state of the tower through the feature vectors is a multi-input single-output and nonlinear problem. LSTM is a class of recurrent neural network (RNN) architecture used to manage the value of long term information, which introduces the gate unit to control the propagation of inputs and outputs.

The state of the cell is determined by the output of each gate at the moment t of the discrete instant, and the order of computation is the forgetting gate f_t , the input gate i_t , and the output gate o_t in that order. σ is the activation function; w is the input-related weight in each gate; w_h is the recursive weight; b is the bias component in each gate; $\hat{c}_t$ denotes the candidate state information in the cell; and tanh is the hyperbolic tangent function. The output value of each gate together with the state information c_{t-1} of the previous cell determines the

state information c_t in the next level cell; and the output gate o_t together with the state information c_t in the next level cell determines the cell-level output information h_t, i.e.:

$$c_t = f_t c_{t-1} + i_t \hat{c}_t \tag{24}$$

$$h_t = o_t \tanh c_t \tag{25}$$

Therefore, when utilizing the LSTM for fault diagnosis, the LSTM will calculate the input signals based on the state information that already exists in a number of cell layers, and derive the corresponding state information h_t.

The establishment of gate units makes LSTM more advantageous for the processing of input information, and when feature vectors are inputted into LSTM, valid and invalid information can be filtered appropriately through the cooperation between gates.

IV. E. Simulation experiment of transmission tower tilt state identification

In this chapter, simulation experiments on transmission tower tilt state identification will be carried out to verify the transmission tower attitude prediction performance of the proposed transmission tower tilt state identification method based on NGO-VMD and LSTM neural network, using GA and QGA as a comparison. The relationship between the fitness function and the number of iterations in the parameter optimization iteration process of this paper's method, GA and QGA is shown in Figure 3. It can be seen that GA optimization algorithm will reach convergence in the 15th iteration, QGA optimization algorithm will reach convergence in the 12th iteration, and the method of this paper will reach convergence in the 5th iteration. Compared with this paper's method, GA and QGA fall into the trap of local optimization, and the convergence speed and prediction accuracy of this paper's method are higher than that of GA and QGA.Therefore, the proposed method of identifying the tilted state of transmission towers based on NGO-VMD and LSTM neural network has better parameter optimization effect than that of GA and QGA, and it can explore the more optimal sparse residuals LSTM neural network's input sparsity rate ISR and implied sparsity rate HSR.

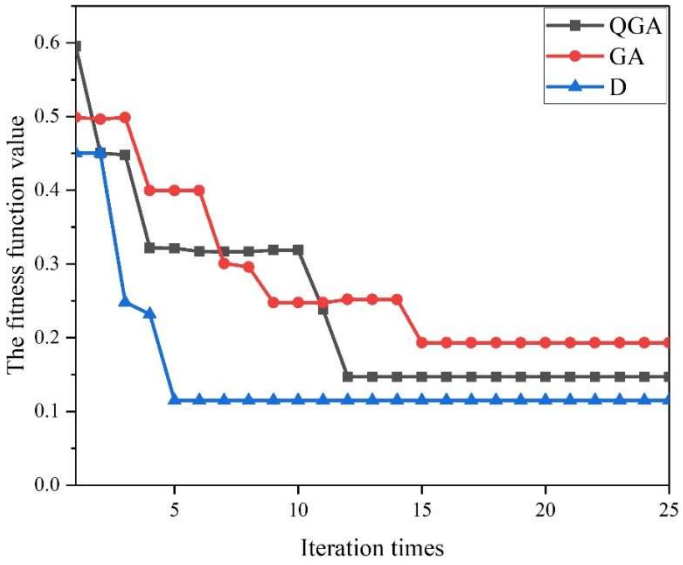

Figure 3: Hyper-parameter optimization iterative process

The transmission tower attitude prediction effects of different transmission tower tilt state recognition methods are shown in Table 3. The average training time in the table refers to the ratio of the training time of all prediction models to the number of prediction models, and the average attitude error refers to the average of the attitude errors of all prediction points. From the data in the table, it can be seen that the average training time and the average attitude error of the transmission tower tilt state recognition method of NGO-VMD and LSTM neural network proposed in this paper are the lowest, reaching 0.396s and 0.119deg, respectively, and are more suitable for the transmission tower tilt state recognition application scenarios that require higher requirements on the timeliness of the prediction and the prediction accuracy.

Table 3: Prediction effects

Prediction method	Average training time (s)	Average attitude error (deg)
RNN	1.732	0.211
LSTM	1.512	0.142
RLSTM	1.243	0.325
GA-SRLSTM	0.958	0.193
QGA-SRLSTM	0.901	0.148
The method of this paper	0.396	0.119

V. Conclusion

The online monitoring system for transmission towers based on IoT platform shows high reliability and practicality in practice. Experimental data show that the system can effectively monitor the tilt angle and environmental parameters of the pole tower with high accuracy. In the static experiments, the Sage-Husa adaptive filtering algorithm significantly reduces the noise of the gyroscope and accelerometer, and the Allan standard deviation of the X, Y, and Z axes are 0.18×10^{-2}, 0.73×10^{-3}, and 0.18×10^{-2}, respectively, which show good noise suppression effects. In the dynamic experiments, the root mean square error (RMSE) of the system is 1.54×10^{-3} °/s and 3.05×10^{-3} m/s², which indicates that the method also has high measurement accuracy in a dynamic environment. Compared with other algorithms, this method has faster convergence speed and higher prediction accuracy, which is suitable for transmission tower monitoring application scenarios that require higher real-time and accuracy.

Acknowledgement

This work was sponsored in part by the Science and Technology Project of State Grid Shanxi Electric Power Company (Grant No. 5205K0240002).

References

[1] Parker, G. G., Tan, B., & Kazan, O. (2019). Electric power industry: Operational and public policy challenges and opportunities. Production and Operations Management, 28(11), 2738-2777.

[2] Seok, K. H., & Kim, Y. S. (2016). A state of the art of power transmission line maintenance robots. Journal of Electrical Engineering and Technology, 11(5), 1412-1422.

[3] Menéndez, O., Pérez, M., & Auat Cheein, F. (2019). Visual-based positioning of aerial maintenance platforms on overhead transmission lines. Applied Sciences, 9(1), 165.

[4] Yongyee, I., Suwanasri, C., Suwanasri, T., & Luejai, W. (2018, March). Condition assessment in transmission line asset for maintenance management. In 2018 International Electrical Engineering Congress (iEECON) (pp. 1-4). IEEE.

[5] Du, W., Wang, J., Yang, G., Zheng, S., & Zhao, Y. (2023). Information Monitoring of Transmission Lines Based on Internet of Things Technology. Scalable Computing: Practice and Experience, 24(2), 115-125.

[6] Judge, M. A., Manzoor, A., Khattak, H. A., Din, I. U., Almogren, A., & Adnan, M. (2021). Secure transmission lines monitoring and efficient electricity management in ultra-reliable low latency industrial internet of things. Computer Standards & Interfaces, 77, 103500.

[7] Suresh, S., Nagarajan, R., Sakthivel, L., Logesh, V., Mohandass, C., & Tamilselvan, G. (2017). Transmission line fault monitoring and identification system by using Internet of Things. International Journal of Advanced Engineering Research and Science (IJAERS), 4(4), 9-14.

[8] Ferreira Dias, C., de Oliveira, J. R., de Mendonça, L. D., de Almeida, L. M., de Lima, E. R., & Wanner, L. (2021). An iot-based system for monitoring the health of guyed towers in overhead power lines. Sensors, 21(18), 6173.

[9] Zhang, X., Zhao, Y., Zhou, L., Zhao, J., Dong, W., Zhang, M., & Lv, X. (2020). Transmission tower tilt monitoring system using low-power wide-area network technology. IEEE Sensors Journal, 21(2), 1100-1107.

[10] Zhao, L., Huang, X., Zhang, Y., Tian, Y., & Zhao, Y. (2019). A vibration-based structural health monitoring system for transmission line towers. Electronics, 8(5), 515.

[11] Tarahi, H., Haghighat, H., Ghandhari, N., & Adinehpour, F. (2022). Smart online protection system for power transmission towers: an IoT-aided design and implementation. IEEE Internet of Things Journal, 10(9), 7480-7489.

[12] Zheng, S., Du, W., Wang, J., Yang, G., & Zhao, Y. (2025). Information Monitoring of Transmission Line Operating Environment based on Internet of Things Technology. Scalable Computing: Practice and Experience, 26(2), 699-707.

[13] Ghasempour, A. (2019). Internet of things in smart grid: Architecture, applications, services, key technologies, and challenges. Inventions, 4(1), 22.

[14] Yao, L. A., Shi, J., Wang, C., Liu, J., & Du, J. (2025). Research on online monitoring system of transmission tower based on computer video algorithm. J. COMBIN. MATH. COMBIN. COMPUT, 124(489), 499.

[15] Fang, J., Zhao, Z., Zhang, J., Luan, T., & Yang, D. (2016). Design of Transmission Tower Inclination Remote Online Monitoring System. International Journal of Simulation--Systems, Science & Technology, 17(30).

[16] Jiang, J. A., Chiu, H. C., Yang, Y. C., Wang, J. C., Lee, C. H., & Chou, C. Y. (2022). On real-time detection of line sags in overhead power grids using an iot-based monitoring system: theoretical basis, system implementation, and long-term field verification. IEEE Internet of Things Journal, 9(15), 13096-13112.

[17] Alias, M. R. N. M., Dzaki, D. R. M., Din, N. M., Deros, S. N. M., Passarella, R., & Chaai, A. E. C. A. (2022, November). Iot-based transmission tower monitoring communications and visualization platform. In 2022 IEEE Symposium on Future Telecommunication Technologies (SOFTT) (pp. 125-129). IEEE.
[18] Long, L. (2022). Research on status information monitoring of power equipment based on Internet of Things. Energy Reports, 8, 281-286.
[19] Wang Zian,Liu Zhigang,Tian Kai & Zhang Huakun. (2023). Frequency-scanning interferometry for dynamic measurement using adaptive Sage-Husa Kalman filter. Optics and Lasers in Engineering,165.
[20] Qilong Wu,Lei Song,Jiarui Huang,Cheng Wang & Xiaochen Jiang. (2024). The Method of Ship Motion Attitude Forecasting based on NGO-VMD and Network Models. International Core Journal of Engineering,10(7).
[21] Shiwei Liu,Xia Hua,Yong Liu,Longxiang Shan,Dongqiao Wang,Qiaohua Wang & Yanhua Sun. (2025). Accurate wire rope defect MFL detection using improved Hilbert transform and LSTM neural network. Nondestructive Testing and Evaluation,40(4),1379-1408.